

## Probing the interface of Fe<sub>3</sub>O<sub>4</sub>/GaAs thin films by hard x-ray photoelectron spectroscopy

M. Paul,<sup>1,\*</sup> A. Müller,<sup>1</sup> A. Ruff,<sup>1</sup> B. Schmid,<sup>1</sup> G. Berner,<sup>1</sup> M. Mertin,<sup>2</sup> M. Sing,<sup>1</sup> and R. Claessen<sup>1</sup>  
<sup>1</sup>Experimentelle Physik 4, Universität Würzburg, D-97074 Würzburg, Germany  
<sup>2</sup>BESSY GmbH, Albert-Einstein-Strasse 15, D-12489 Berlin, Germany

(Received 16 March 2009; revised manuscript received 7 May 2009; published 4 June 2009)

Magnetite (Fe<sub>3</sub>O<sub>4</sub>) thin films on GaAs have been studied with hard x-ray photoelectron spectroscopy (HAXPES) and low-energy electron diffraction. Films prepared under different growth conditions are compared with respect to stoichiometry, oxidation, and chemical nature. Employing the considerably enhanced probing depth of HAXPES as compared to conventional x-ray photoelectron spectroscopy allows us to investigate the chemical state of the film-substrate interfaces. The degree of oxidation and intermixing at the interface are dependent on the applied growth conditions; in particular, we found that metallic Fe, As<sub>2</sub>O<sub>3</sub>, and Ga<sub>2</sub>O<sub>3</sub> exist at the interface. These interface phases might be detrimental for spin injection from magnetite into GaAs.

DOI: [10.1103/PhysRevB.79.233101](https://doi.org/10.1103/PhysRevB.79.233101)

PACS number(s): 79.60.Jv, 79.60.Dp

The ferrimagnetic iron oxide magnetite (Fe<sub>3</sub>O<sub>4</sub>) is ranked among the most attractive materials for the currently developing field of spintronics.<sup>1</sup> The basic concept of spintronics consists in the design of integrated circuits which use the electron *spin* for data storage and processing of information.<sup>2</sup> In spintronic devices, semiconducting materials, used in conventional charge-based electronic chips, and ferromagnetic materials, employed in storage devices, are combined in a new way. Therefore a key element is the integration of magnetic materials such as metallic ferromagnets, diluted magnetic semiconductors, or oxidic half-metallic ferromagnets with substrates used in existing semiconductor technology. Magnetite stands out from other feasible magnetic materials due to the following bulk material characteristics: a very high Curie temperature of 858 K, a predicted spin polarization of  $-100\%$  (minority spins only) at the Fermi level,<sup>3</sup> and a conductivity of  $2.5 \times 10^4$  ( $\Omega \text{ m}$ )<sup>-1</sup> at room temperature<sup>4</sup> which matches quite well the value of semiconducting materials. For a film/substrate structure without buffer layer, the latter two features are crucial to facilitate spin injection into the semiconducting host via an Ohmic contact.<sup>5</sup> However, the experimentally substantiated spin polarization of Fe<sub>3</sub>O<sub>4</sub> is lower and ranges from  $-55\%$  (Refs. 6–8) for the free (100) surface to  $-80\%$  (Ref. 9) for the free (111) surface.

Hence there exists a clear need to study the growth behavior and thin-film properties of magnetite on semiconducting substrates such as GaAs. Moreover, a detailed knowledge of the actual interface structure and stoichiometry is desirable in order to correlate it with the magnetic and spin transport properties. Interface issues as the occurrence of mixed phases could prevent a successful growth or at least influence material properties in an undesired way, e.g., limit the degree of spin polarization at near-interface layers or surfaces.

Previous work done on thin-film growth of Fe<sub>3</sub>O<sub>4</sub> mostly utilized oxide substrates. Recent interest has been directed at the use of semiconducting substrates.<sup>10–15</sup> However, there are only sparse experimental reports<sup>10,13</sup> on interface chemistry and interface reactions, although based on thermodynamic considerations such interfaces might not be stable.<sup>16</sup>

In this work, we examine this problem and investigate the chemical nature of Fe<sub>3</sub>O<sub>4</sub> films grown on GaAs(100) substrates and their respective interfaces. Hard x-ray photoelec-

tron spectroscopy (HAXPES) is an ideal tool to study the electronic structure and chemical state of these films. In particular, the larger information depth due to photon energies in the hard x-ray regime allows us to probe the interface between film and substrate in a nondestructive way. Changing the photon energy while looking at the same core level permits for depth profiling of the sample with respect to the specific element or chemical species under consideration. To give numbers, the inelastic mean-free path of photoelectrons increases from 38 to 51 Å, from 32 to 46 Å, and from 30 to 43 Å for the Fe 2p<sub>3/2</sub>, Ga 2p<sub>3/2</sub>, and As 2p<sub>3/2</sub> core levels, respectively, upon changing the photon energy from 3 to 4 keV.<sup>17</sup> Fe<sub>3</sub>O<sub>4</sub>/GaAs(100) samples were grown in a ultrahigh-vacuum chamber equipped with an electron-beam evaporator with a built-in flux meter, a gas inlet system for oxygen of ultrahigh purity, and a low-energy electron-diffraction (LEED) optics for surface monitoring. Beforehand GaAs substrates were cut from a Si- (*n*-) doped wafer, etched with highly concentrated sulphuric acid and rinsed with de-ionized water, both under flowing conditions. As an *in situ* treatment sample 1 was sputtered (Ar<sup>+</sup>, energy of 1 keV) and annealed to 820 K, while sample 2 was annealed only to 770 K prior to actual film growth. As we verified by x-ray photoelectron spectroscopy (XPS) measurements these substrate treatments result in clean GaAs without its native oxides. The following growth conditions were applied: Fe film growth at room temperature and postoxidation at 700 K and  $p(\text{O}_2) = 1 \times 10^{-6}$  mbar for 30 min (sample 1) and at 600 K and  $p(\text{O}_2) = 5 \times 10^{-5}$  mbar for 3 min (sample 2). The deposited Fe film thickness was 23 Å (sample 1) and 36 Å (sample 2), respectively, as derived from the flux meter calibrated against a quartz-crystal monitor.

A typical LEED pattern of a cleaned GaAs(100) substrate, which exhibits the  $1 \times 1$  surface unit cell, is displayed in Fig. 1(a). On such substrate surfaces, Fe, which is known to grow epitaxially on GaAs(100),<sup>18</sup> was deposited at room temperature. As is known from the literature the growth mode depends on the substrate reconstruction and temperature and is, e.g., three dimensional on Ga-rich GaAs(100)-*c*( $8 \times 2$ ) with islands coalescing above four monolayers<sup>19</sup> or predominantly layer by layer on As-rich GaAs(100)-( $2 \times 4$ ).<sup>20</sup> The epitaxial growth of Fe in our case was confirmed by good quality

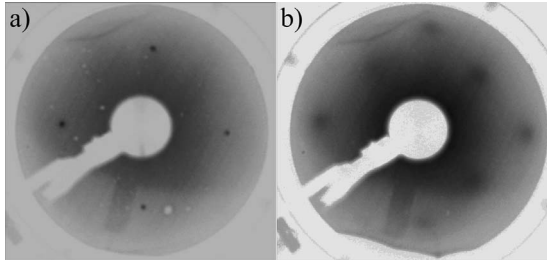


FIG. 1. (a) Typical LEED pattern of a GaAs substrate showing the  $1 \times 1$  surface unit cell;  $E=35.9$  eV. (b) LEED pattern of a  $\text{Fe}_3\text{O}_4$  thin film (sample 1) showing the  $1 \times 1$  surface unit cell corresponding to the O sublattice;  $E=89.0$  eV.

LEED patterns (not shown here). LEED images of Fe films postoxidized to  $\text{Fe}_3\text{O}_4$  [see Fig. 2(b)] show a square unit cell with a lattice constant of about 3 Å. Additional spots were not present. Naively, one would expect a lattice constant of 5.9 Å for magnetite (corresponding to a  $2 \times 2$  unit cell with respect to the observed one) or a  $(\sqrt{2} \times \sqrt{2})R45^\circ$  superstructure, giving rise to a lattice constant of 8.4 Å. The latter is typically observed for magnetite single crystals or thicker films. Since the  $(\sqrt{2} \times \sqrt{2})R45^\circ$  superstructure is due to the polar nature of the  $\text{Fe}_3\text{O}_4$  stacking sequence, its absence can be related to the very small film thickness. We are thus led to interpret the observed  $1 \times 1$  unit cell with a lattice constant of roughly 3 Å as signature of the oxygen sublattice, which is common to all Fe oxides ( $\text{FeO}$ ,  $\text{Fe}_3\text{O}_4$ ,  $\text{Fe}_2\text{O}_3$ ). The main reason for the missing  $2 \times 2$  and the observed broad diffraction spots might be disorder due to amorphous interface phases.

HAXPES experiments were carried through at room temperature and without further surface treatment to avoid a change in chemical composition using beamline KMC-1 at BESSY in Berlin. The total-energy resolutions were 0.74 and 0.90 eV at photon energies of 3 and 4 keV, respectively, as were checked by measuring the Au  $4f_{7/2}$  core level with an intrinsic linewidth of 0.25 eV (full width at half maximum). The shown spectra have been shifted to correct for charging by setting the O  $1s$  binding energy to 530.1 eV which is known to be the same in all Fe oxides.<sup>21</sup>

In Fig. 2 core-level spectra measured with photon energies of 3 and 4 keV on samples 1 and 2 are shown. The Ga  $2p_{3/2}$  level [see Fig. 2(a)] is composed of a main compo-

nent due to GaAs at  $1116.9 \pm 0.2$  eV binding energy, which matches perfectly the literature value for GaAs,<sup>22</sup> and a smaller oxide peak at 1.3 eV higher binding energy, which appears in the 3 keV spectrum as small shoulder and is hardly visible in the spectrum taken with 4 keV photons. Due to its chemical shift with respect to the main line, the oxide peak can be attributed to  $\text{Ga}_2\text{O}_3$ .<sup>22</sup> The main component due to GaAs is enhanced in the 4 keV spectrum with higher information depth while the oxide component is stronger in the more surface and interface sensitive spectrum.

Similar conclusions can be drawn in the case of the As  $2p_{3/2}$  core level shown in Fig. 2(b). Here the main component has a binding energy of  $1322.4 \pm 0.1$  eV, which is comparable to the literature,<sup>22</sup> where values of 1322.8 eV for GaAs and 1322.4 eV for elemental As are reported. Taking into account the relevant photoionization cross sections, asymmetry parameters, inelastic electron mean-free paths, and the analyzer transmission function, the intensity ratios of the Ga  $2p_{3/2}$  to the As  $2p_{3/2}$  main component range from 0.82 to 0.98 for different samples and photon energies and are therefore close to the ideal stoichiometry for GaAs. On this account we assign the As  $2p_{3/2}$  main component to GaAs and not to elemental As since there is no indication for a significant off-stoichiometric amount of excess As with respect to Ga. After having identified the As  $2p_{3/2}$  main component, an additional component or shoulder is indeed not seen at a chemical shift of 0.6 eV (Refs. 23 and 24) higher binding energy, which then would indicate elemental As. The oxide As  $2p_{3/2}$  component appears at 3.1 eV higher binding energies and hence can be attributed to  $\text{As}_2\text{O}_3$ .<sup>22</sup> The main component due to GaAs is enhanced in the 4 keV spectrum with higher information depth while the oxide component is stronger in the more surface and interface sensitive spectrum.

As has been mentioned above, the O  $1s$  main peak (not shown here) serves as energy reference with a binding energy of 530.1 eV. We also find a feature at 1.6 eV higher binding energy which presumably stems from OH groups at the surface<sup>25</sup> since it decreases upon changing the photon energy from 3 to 4 keV. This contribution obviously reflects the amount of contamination due to exposure to air and is not related to sample preparation conditions.

In Figs. 2(c) and 2(d) the Fe  $2p$  spectra of samples 1 and 2 are depicted. Concentrating on the more intense Fe  $2p_{3/2}$  part of the spectrum, for sample 1 [see Fig. 2(c)], one can clearly distinguish two spectral features: the main component

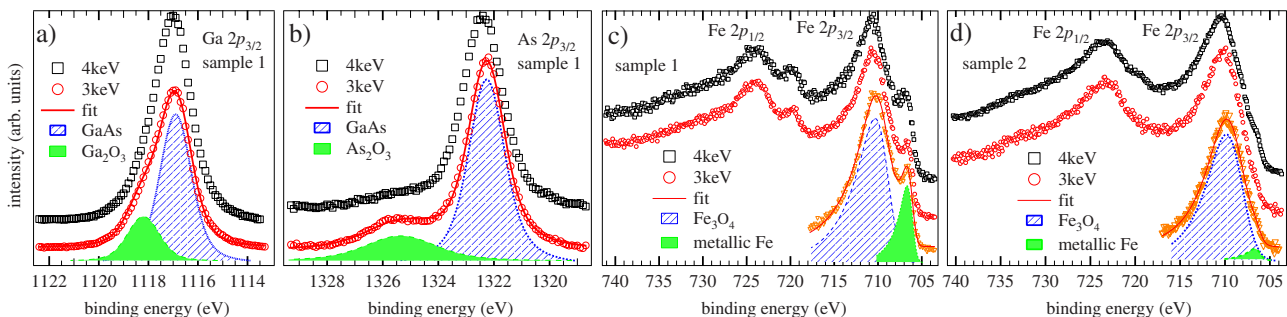


FIG. 2. (Color online) HAXPES core-level spectra of  $\text{Fe}_3\text{O}_4/\text{GaAs}$  samples taken with  $h\nu=3$  and 4 keV; also shown are the decomposition of the spectra in various components according to a fitting procedure and the resulting fit curves; curves are shifted in vertical direction for clarity. (a) Sample 1: Ga  $2p_{3/2}$ , (b) sample 1: As  $2p_{3/2}$ , (c) sample 1: Fe  $2p$ , and (d) sample 2: Fe  $2p$ .

TABLE I. XPS signal of different chemical species normalized to the total XPS signal for that element.

Species	Sample 1		Sample 2	
	3 keV	4 keV	3 keV	4 keV
As: $\text{As}_2\text{O}_3/(\text{As}_2\text{O}_3+\text{GaAs})$	0.21	0.08	0.07	0
Ga: $\text{Ga}_2\text{O}_3/(\text{Ga}_2\text{O}_3+\text{GaAs})$	0.23	0.11	0.10	0.02
Fe: $\text{Fe}/(\text{Fe}+\text{Fe}_3\text{O}_4)$	0.19	0.23	0.04	0.07
O: $\text{OH}(\text{surface})/(\text{OH}+\text{oxide})$	0.79	0.77	0.57	0.32

at  $710.1 \pm 0.3$  eV and a smaller peak at the lower-binding-energy side of the main line, shifted by 3.6 eV. The main component is readily attributed to  $\text{Fe}_3\text{O}_4$ , while the second peak is due to metallic Fe. The same oxidation states ( $\text{Fe}_3\text{O}_4$ , Fe) are reflected in the Fe  $2p_{1/2}$  line at binding energies of about 723.5 and 720 eV. Corresponding spectral features are discerned in the Fe  $2p$  spectrum of sample 2 [see Fig. 2(d)] although the metallic Fe-related features appear here only as weak shoulders of the main lines. For both samples the metallic component is stronger in the spectrum taken at higher photon energy, i.e., with larger information depth. Since the amount of metallic Fe in sample 2 was too small to be detected by conventional XPS using monochromated Al  $K\alpha$  radiation (1486.6 eV), we conclude that the metallic Fe is not located at the surface but deeper in the bulk, probably at or near to the interface. The spectrum taken at  $h\nu=3$  keV on sample 2 exhibits only a marginal contribution of metallic Fe and hence displays most clearly the overall spectral shape of the mixed-valence state of  $\text{Fe}_3\text{O}_4$  (Ref. 21): the  $2p_{3/2}$  peak lies roughly at 710.5 eV and the structure between the spin-orbit split peaks is smeared out. In case of  $\text{Fe}_2\text{O}_3$  the  $\text{Fe}^{3+}$  charge-transfer satellite should be visible at 719 eV, and for FeO the  $\text{Fe}^{2+}$  satellite should appear at 715.5 eV. Both signatures are not seen here.

To quantify our results, for each element its relative amount in a certain chemical species as derived from numerical fits (see Fig. 2) is summarized in Table I. The values support the statement that the oxides  $\text{Ga}_2\text{O}_3$  and  $\text{As}_2\text{O}_3$  are located at the interface or at least nearer to the surface, while the metallic Fe is situated deeper in the bulk or at the interface. The OH groups are adsorbed at the surface.

Assuming a layered structure of the samples, we can calculate the thicknesses of the As and Ga oxide layers at the interface using the equation in Ref. 26 (see also Ref. 24) from the ratios in Table I. The  $\text{As}_2\text{O}_3$  layer thickness amounts to  $4.9 \pm 1.6$  and  $1 \pm 1$  Å and the  $\text{Ga}_2\text{O}_3$  layer thickness to  $4.0 \pm 1.0$  and  $1.2 \pm 0.7$  Å for samples 1 and 2, respectively. The thicknesses for both investigated samples differ substantially and are only about one monolayer for sample 2. We finally arrive at a dimensioned sketch of the vertical structures and compositions of samples 1 and 2 displayed in Fig. 3.

To better understand the results at hand concerning As and Ga oxides, we recall some experimental findings on the oxidation of GaAs surfaces. Experiments on the thermal oxidation of GaAs have shown that at high temperatures (800–1000 K) primarily polycrystalline  $\text{Ga}_2\text{O}_3$  and possibly

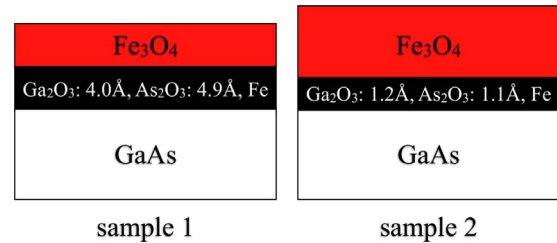


FIG. 3. (Color online) Simplified sketch of the proposed vertical sample structures with phases and layer thicknesses as indicated.

$\text{GaAsO}_4$  are formed.<sup>23,27</sup> At lower oxidation temperatures the resulting products are amorphous and again mainly  $\text{Ga}_2\text{O}_3$  and a smaller fraction of elemental As at the oxide/GaAs interface.  $\text{As}_2\text{O}_3$  is additionally found for oxidation with molecular oxygen at low and intermediate temperatures. Transferring these results to our case, the oxidation conditions for the GaAs substrate in  $\text{Fe}_3\text{O}_4/\text{GaAs}$  apparently are weak because of rather low temperatures, small oxygen partial pressure, and the presence of the easily oxidized Fe. In accordance, no  $\text{GaAsO}_4$  has been observed which could easily be detected by XPS due to the large chemical shift of about  $-4.8$  eV with respect to the GaAs component in both As and Ga core levels. On the other hand, given weak oxidation conditions, elemental As should be found, which we do not. Probably the formation of elemental As is hindered by kinetic factors in our case.

Former publications<sup>10,12–15</sup> on  $\text{Fe}_3\text{O}_4/\text{GaAs}$  samples cover their fabrication by postoxidation as in this study,<sup>11</sup> pulsed laser deposition (PLD),<sup>10</sup> reactive dc magnetron sputtering from Fe in an  $\text{O}_2$  partial pressure,<sup>12</sup> and reactive molecular-beam epitaxy (MBE).<sup>15</sup> However, the latter two publications<sup>12,15</sup> do not report if interface phases exist after the application of their respective growth method, which hampers a direct comparison with present results. Lu *et al.*<sup>11</sup> found that  $\text{Fe}_3\text{O}_4$  grows (100) oriented on GaAs(100) when postoxidizing a Fe film grown by MBE. Interestingly, they have measured an Fe  $2p$  spectrum by conventional XPS indicating small amounts of metallic Fe, similar to what we find, but this fact was not commented there.<sup>11</sup> However, in a later x-ray magnetic circular dichroism study<sup>28</sup> on similarly prepared samples, they did not confirm the presence of metallic Fe and reported instead that, above a critical  $\text{Fe}_3\text{O}_4$  film thickness of 3 nm, a FeO interface layer forms and increases with film thickness. The presence of interfacial FeO was attributed to oxygen defects. We note that the presence of interfacial FeO can also be explained with an interface reaction between  $\text{Fe}_3\text{O}_4$  and GaAs producing FeO and Ga and As oxides, similar to our case.

Preisler *et al.*<sup>10</sup> proposed that their obtained (111)-oriented polycrystalline growth of  $\text{Fe}_3\text{O}_4$  on GaAs(100) by means of PLD is triggered by the presence of an amorphous interface. Moreover, they saw a strong shoulder in the XPS Ga  $3d$  spectrum measured with Al  $K\alpha$  radiation indicating Ga-Fe bonding. We clearly do not see evidence for a (111) orientation, a polycrystalline film structure, or Ga-Fe bonding in our results. However, the moderate quality of the obtained LEED patterns of our very thin films could be linked to the presence of amorphous Ga and As oxide interface phases. The finding

of a Ga-Fe species by Preisler *et al.* can be explained by a stronger intermixing and a reduction in Fe<sub>3</sub>O<sub>4</sub> to Fe at the interface which in turn could be induced by the use of the PLD technique.

With the future application of Fe<sub>3</sub>O<sub>4</sub>/GaAs in spintronics in mind, the influence of interface phases such as Fe, As<sub>2</sub>O<sub>3</sub>, and Ga<sub>2</sub>O<sub>3</sub> on the magnetic properties of Fe<sub>3</sub>O<sub>4</sub> films is an important issue which demands for further investigations. It has, e.g., been shown that an Fe<sub>3</sub>O<sub>4</sub>/Fe bilayer possesses antiparallel magnetic coupling.<sup>29</sup> Further, a metallic interface layer with high conductivity is expected to decrease the efficiency of spin injection considerably.<sup>5</sup> At last, As<sub>2</sub>O<sub>3</sub> and Ga<sub>2</sub>O<sub>3</sub> could act as a spin-injection tunneling barrier for the spin-polarized electrons. Concerning the latter point, from our results, postoxidation of the Fe films at lower temperatures seems favorable since it results in considerably smaller thicknesses of the interfacial oxide layer (see Fig. 3).

In summary, we have demonstrated the successful growth

of Fe<sub>3</sub>O<sub>4</sub> films on the semiconducting substrate GaAs(100) and have characterized them through depth-resolved investigation of the chemical nature of film and interface regions. An oxidation of GaAs to As<sub>2</sub>O<sub>3</sub> and Ga<sub>2</sub>O<sub>3</sub> near the interface and a simultaneous reduction in Fe<sub>3</sub>O<sub>4</sub> to Fe has been revealed. For a lower growth temperature of 600 K, the amounts of oxidized GaAs and metallic Fe were less compared with postoxidation at 700 K. As has been demonstrated, HAXPES is a useful and essential method for the depth-resolved characterization of chemical phases in thin-film structures and is superior to conventional XPS for the identification of interface phases.

The authors thank A. Gloskovskij, F. Casper, J. Barth, and S. Tabor for their experimental support during beam times at BESSY. They acknowledge financial support by BMBF through Project No. 05 KS7WW3. M.P. acknowledges financial support by DAAD.

\*paul@physik.uni-wuerzburg.de

- <sup>1</sup>A. M. Haghiri-Gosnet, T. Arnal, R. Soulimane, M. Koubaa, and J. P. Renard, *Phys. Status Solidi A* **201**, 1392 (2004).
- <sup>2</sup>S. A. Wolf, D. D. Aschwalom, R. A. Buhrman, J. M. Daughton, S. von Molnar, M. L. Roukes, A. Y. Chtchelkanova, and D. M. Treger, *Science* **294**, 1488 (2001).
- <sup>3</sup>A. Yanase and N. Hamada, *J. Phys. Soc. Jpn.* **68**, 1607 (1999).
- <sup>4</sup>P. A. Miles, W. B. Westphal, and A. von Hippel, *Rev. Mod. Phys.* **29**, 279 (1957).
- <sup>5</sup>G. Schmidt, D. Ferrand, L. W. Molenkamp, A. T. Filip, and B. J. van Wees, *Phys. Rev. B* **62**, R4790 (2000).
- <sup>6</sup>S. F. Alvarado, M. Erbudak, and P. Munz, *Phys. Rev. B* **14**, 2740 (1976).
- <sup>7</sup>S. A. Morton, G. D. Waddill, S. Kim, I. K. Schuller, S. A. Chambers, and J. G. Tobin, *Surf. Sci.* **513**, L451 (2002).
- <sup>8</sup>M. Fonin, R. Pentcheva, Y. S. Dedkov, M. Sperlich, D. V. Vyalikh, M. Scheffler, U. Rüdiger, and G. Güntherodt, *Phys. Rev. B* **72**, 104436 (2005).
- <sup>9</sup>Y. S. Dedkov, U. Rüdiger, and G. Güntherodt, *Phys. Rev. B* **65**, 064417 (2002).
- <sup>10</sup>E. J. Preisler, J. Brooke, N. C. Oldham, and T. C. McGill, *J. Vac. Sci. Technol. B* **21**, 1745 (2003).
- <sup>11</sup>Y. X. Lu, J. S. Claydon, Y. B. Xu, S. M. Thompson, K. Wilson, and G. van der Laan, *Phys. Rev. B* **70**, 233304 (2004).
- <sup>12</sup>S. M. Watts, K. Nakajima, S. van Dijken, and J. M. D. Coey, *J. Appl. Phys.* **95**, 7465 (2004).
- <sup>13</sup>S. Jain, A. O. Adeyeye, and C. B. Boothroyd, *J. Appl. Phys.* **97**, 093713 (2005).
- <sup>14</sup>M. Ferhat and K. Yoh, *Appl. Phys. Lett.* **90**, 112501 (2007).
- <sup>15</sup>T. Taniyama, T. Mori, K. Watanabe, E. Wada, M. Itoh, and H. Yanagihara, *J. Appl. Phys.* **103**, 07D705 (2008).
- <sup>16</sup>K. J. Hubbard and D. G. Schlom, *J. Mater. Res.* **11**, 2757 (1996).
- <sup>17</sup>S. Tanuma, T. Shiratori, T. Kimura, K. Goto, S. Ichimura, and C. J. Powell, *Surf. Interface Anal.* **37**, 833 (2005).
- <sup>18</sup>Y. B. Xu, E. T. M. Kernohan, D. J. Freeland, A. Ercole, M. Tselepi, and J. A. C. Bland, *Phys. Rev. B* **58**, 890 (1998).
- <sup>19</sup>S. A. Chambers, F. Xu, H. W. Chen, I. M. Vitomirov, S. B. Anderson, and J. H. Weaver, *Phys. Rev. B* **34**, 6605 (1986).
- <sup>20</sup>E. Kneedler, P. M. Thibado, B. T. Jonker, B. R. Bennett, L. J. Whitman, B. V. Shanabrook, and J. J. Krebs, *J. Appl. Phys.* **79**, 5125 (1996).
- <sup>21</sup>S. Gota, J. B. Moussy, M. Henriot, M. J. Guittet, and M. Gautier-Soyer, *Surf. Sci.* **482–485**, 809 (2001).
- <sup>22</sup>J. Massies and J. P. Contour, *J. Appl. Phys.* **58**, 806 (1985).
- <sup>23</sup>G. Hollinger, R. Skheyta-Kabbani, and M. Gendry, *Phys. Rev. B* **49**, 11159 (1994).
- <sup>24</sup>Z. Liu, Y. Sun, F. Machuca, P. Pianetta, W. E. Spicer, and R. F. W. Pease, *J. Vac. Sci. Technol. A* **21**, 212 (2003).
- <sup>25</sup>P. Liu, T. Kendelewicz, G. E. Brown, E. J. Nelson, and S. A. Chambers, *Surf. Sci.* **417**, 53 (1998).
- <sup>26</sup> $d_{ov} = \lambda_{sub} \cos \theta \ln \left( \frac{D_{sub} I_{ov}}{D_{ov} I_{sub}} + 1 \right)$  where  $\lambda_{sub}$  is the electron mean-free path,  $\theta$  is the electron emission angle from the surface normal,  $I_{ov}$  and  $I_{sub}$  are the XPS peak intensities of overlayer (oxide) and substrate level, and  $D_{ov}$  and  $D_{sub}$  are the atomic densities of the element in overlayer and substrate in mol/cm<sup>3</sup>.
- <sup>27</sup>C. W. Wilmsen, *J. Vac. Sci. Technol.* **19**, 279 (1981).
- <sup>28</sup>Y. X. Lu, J. S. Claydon, E. Ahmad, Y. B. Xu, S. M. Thompson, K. Wilson, and G. van der Laan, *IEEE Trans. Magn.* **41**, 2808 (2005).
- <sup>29</sup>H.-J. Kim, J.-H. Park, and E. Vescovo, *Phys. Rev. B* **61**, 15288 (2000).